

# A Study on Heat Transfer of Cu-Water Nanofluid in a 2D Inclined Porous Cavity using COMSOL Multiphysics

Nur Haidah Izzati Abu<sup>1</sup>, Muhamad Ghazali Kamardan<sup>1\*</sup>

<sup>1</sup> Department of Mathematics and Statistics, Faculty of Applied Science and Technology, UTHM Kampus Cawangan Pagoh, Hab Pendidikan Tinggi Pagoh, KM 1, Jalan Panchor, 84600 Pagoh, Muar, Johor, MALAYSIA

\*Corresponding Author: [mghazali@uthm.edu.my](mailto:mghazali@uthm.edu.my)

DOI: <https://doi.org/10.30880/ekst.2024.04.01.009>

## Article Info

Received: 27 December 2023

Accepted: 03 June 2024

Available online: 27 July 2024

## Keywords

Natural Convection, COMSOL Multiphysics, Porous media, isotherms, streamlines

## Abstract

This study examined the heat transfer of Cu-water nanofluid in a 2D inclined porous cavity. The horizontal walls are perfectly insulated and the vertical walls have different temperatures. The streamlines and isotherms were analyzed using COMSOL Multiphysics. Darcy-Brinkman-Forchheimer equations has been modeled as a transport equation for nanofluid saturated porous medium. The influence of non-dimensional parameter such as inclination angle was studied. The results obtained the magnitude of the inclination angle and the variety of wall positions change because of that are rich in fluid dynamics in the cavity.

## 1. Introduction

Natural convection is a type of heat transfer by movement of the fluid due to the temperature variation in the fluid and the corresponding variation in density [1-2]. Natural convection has been employed in the industry, solar energy collectors, agriculture, nuclear energy, telecommunication and aviation [3]. With the practical point of view some of papers, natural convection is a broad physical phenomenon whose behavior is divided into two primary types according to the direction of the temperature gradient with regard to gravity. It has applications in both engineering and natural processes. Natural convection is classified into two main classes. The first class involves a temperature gradient aligned with the direction of gravity, where hot air rises and cooler air sinks vertically. The second class features a temperature gradient orthogonal to the direction of gravity, leading to temperature changes along a horizontal surface [4].

In the past several decades there is a lot of studies investigated about natural convection in an inclined angle. One of these researches, the author studied about the natural convection in an inclined enclosure with cooling at the bottom wall. Their result shown Rayleigh number always depends on heat flow. The higher the heat flow, the higher the Rayleigh number and vice versa [5]. Other than that, the researcher investigated the effect of inclination on flow mode transition using the Boussinesq equation. They found the sensitivity of the initial conditions on flow pattern formation [6]. In addition, there are also studies that use the Darcy's law and the Boussinesq approximation to explore entropy formation in an inclined porous cavity for natural convection. The study found that when the Rayleigh number decreases, the dominance of heat transfer over fluid friction also decreases [7]. Lastly, the researcher explored a strong magnetic field in a porous medium-filled inclined enclosure. When the Darcy number is small, conduction dominance is observed with the average Nusselt number indicating a transition point with a stronger magnetic field [8].

There are also many researchers who use COMSOL Multiphysics as a software to solve problems in natural convection. One of the researchers conducted an investigation focused on different factors such as Rayleigh number, heater location, magnetic dipole strength, and horizontal/vertical positions of the magnetic dipole. The results found that increasing the strength of the magnetic dipole resulted in a decrease in the average heat

transfer while adjusting the horizontal position led to an increase in the average heat transfer [9]. Another study investigated natural convection in an air-filled polygonal enclosure, revealing that increased polygonal sides reduced the Nusselt number, and larger cylinder diameters caused a reduction in the Nusselt number [10].

This study examined the heat transfer of Cu-water nanofluid in a 2D inclined porous cavity using COMSOL Multiphysics. The bottom and top walls were perfectly insulated while for the right and left walls, the temperature was constant. Previous research has investigated the impact of internal heat generation in porous cavities containing Cu-water nanofluids on unstable laminar convection [11]. This study is an extension of the research conducted by Rajarathinam [11], and we use Dirichlet boundary conditions to express the results. Darcy number and inclination angle are analyzed using COMSOL Multiphysics and the effect of heat transfer in porous cavity filled with nanofluid are shown in streamline and isotherms.

#### Nomenclature

|        |  |
|--------|--|
| $C_p$  | specific heat                          |
| $Da$   | Darcy number                           |
| $Fc$   | Forchheimer coefficient                |
| $g$    | gravitational acceleration vector      |
| $k$    | thermal conductivity                   |
| $K$    | permeability                           |
| $L$    | length of cavity                       |
| $p$    | fluid pressure                         |
| $P$    | non-dimension pressure                 |
| $Pr$   | Prandtl number                         |
| $q$    | uniform volumetric heat generation     |
| $Q$    | non-dimension internal heat generation |
| $Ra$   | Rayleigh number                        |
| $t$    | time                                   |
| $T$    | temperature                            |
| $T_h$  | temperature hot                        |
| $T_c$  | temperature cold                       |
| $u, v$ | velocity components in x, y directions |
| $U, V$ | non-dimension velocity                 |
| $x, y$ | cartesian coordinates                  |
| $X, Y$ | non-dimension coordinates              |

#### Greek symbols

|            |                               |
|------------|-------------------------------|
| $\alpha$   | thermal diffusivity           |
| $\beta$    | thermal expansion coefficient |
| $\gamma$   | inclination angle             |
| $\theta$   | non-dimension temperature     |
| $\epsilon$ | porosity                      |
| $\phi$     | solid volume fraction         |
| $\sigma$   | specific heat ratio           |
| $\mu$      | dynamic viscosity             |
| $\nu$      | kinematic viscosity           |
| $\rho$     | density                       |
| $\tau$     | non-dimension time            |

#### Subscripts

|      |              |
|------|--------------|
| $c$  | cold         |
| $f$  | fluid        |
| $h$  | hot          |
| $nf$ | nanofluid    |
| $p$  | nanoparticle |
| $s$  | solid phase  |

## 2. Methodology

### 2.1 Mathematical formulation

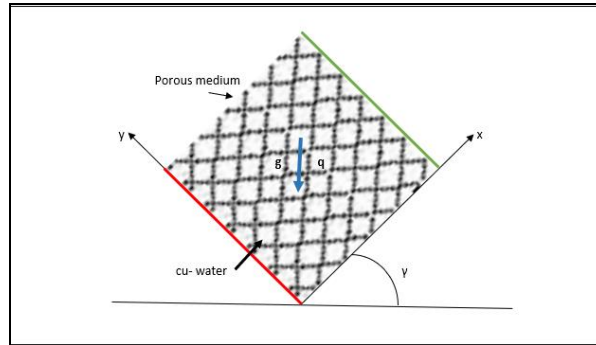


**Fig. 1** Figure description schematic of the physical situation [9]

Fig 1 represented the problem of a two-dimensional porous square cavity of size  $L$  filled with a Cu-water nanofluid that generates heat at a constant volumetric heat rate. The cavity has an angle of with regard to the horizontal plane at an angle of  $\gamma$ . The porous medium is homogeneous and isotropic and in thermal between the fluid and solid phase. Porous medium fills the entire cavity. At the right wall is cold while at the left wall is hot. At the bottom and top walls were perfectly insulated. The Darcy-Brinkmann-Forchheimer model was used to analyzed fluid saturated porous medium. Darcy law is an equation that describe about flow in porous medium while Brinkmann and Forchheimer was modification of Darcy law. It is considered that there is no slip between the base fluid and the nanoparticles and that they are in thermal equilibrium.

**Table 1** Thermo-physical characteristics of Cu nanoparticles with base fluid water

| Physical characteristics | Fluid phase (Water) | Cu   |
|--------------------------|---------------------|------|
| $C_p$ (J/kg K)           | 4179                | 385  |
| $K$ (W/m K)              | 0.613               | 401  |
| $P$ (kg/m <sup>3</sup> ) | 997.1               | 8933 |

Table 1 shows the thermo-physical characteristics of cu nanoparticles with base fluid water. The value of specific heat, thermal conductivity and density for fluid phase and cu-water is presented. These values will be input in COMSOL Multiphysics to perform the analysis.

The governing equations for the system are:

$$\frac{\partial u}{\partial x} + \frac{\partial v}{\partial y} = 0 \quad (1)$$

$$\frac{1}{\varepsilon} \frac{\partial u}{\partial t} + \frac{1}{\varepsilon^2} \left( u \frac{\partial u}{\partial x} + v \frac{\partial u}{\partial y} \right) = -\frac{1}{\rho_{nf}} \frac{\partial p}{\partial x} + \frac{v_{nf}}{\varepsilon} \nabla^2 u - \frac{v_{nf}}{K} u - \frac{Fc}{\sqrt{K}} u \sqrt{u^2 + v^2} + \sin \gamma g \beta_{nf} (T - T_c) \quad (2)$$

$$\frac{1}{\varepsilon} \frac{\partial v}{\partial t} + \frac{1}{\varepsilon^2} \left( u \frac{\partial v}{\partial x} + v \frac{\partial v}{\partial y} \right) = -\frac{1}{\rho_{nf}} \frac{\partial p}{\partial y} + \frac{v_{nf}}{\varepsilon} \nabla^2 v - \frac{v_{nf}}{K} v - \frac{Fc}{\sqrt{K}} v \sqrt{u^2 + v^2} + \cos \gamma g \beta_{nf} (T - T_c) \quad (3)$$

$$\sigma \frac{\partial T}{\partial t} + \left( u \frac{\partial T}{\partial x} + v \frac{\partial T}{\partial y} \right) = \frac{k_{nf}}{(\rho c_p)_{nf}} \nabla^2 T + \frac{q}{(\rho C_p)_{nf}} (T - T_c) \quad (4)$$

Where  $F_c = \frac{175}{\sqrt{150\varepsilon^2}}$  is the Forchheimer coefficient.

The initial and boundary conditions are as follow:

$$\begin{aligned} t = 0 : u = v = 0, T = T_c, 0 \leq X \leq L, 0 \leq Y \leq L \\ t > 0 : u = v = 0, T = T_h, X = 0, 0 \leq Y \leq L \\ u = v = 0, T = T_c, X = L, 0 \leq Y \leq L \\ u = v = 0, \frac{\partial T}{\partial Y} = 0, Y = 0 \& L, 0 \leq X \leq L \end{aligned}$$

The dimensionless variables are as the following:

$$(X, Y) = \frac{(x, y)}{L} \quad (U, V) = \frac{(u, v)}{\frac{\alpha_f}{L}}, \quad \tau = \frac{\alpha_f t}{L^2}, \quad P = \frac{\rho L^2}{\rho_{nf} \alpha_f^2}, \quad \theta = \frac{T - T_c}{T_h - T_c}$$

Using the non-dimensional variables, the Eqs (1)-(4) can be rewritten in the form of non-dimension equation as

$$\frac{\partial U}{\partial X} + \frac{\partial V}{\partial Y} = 0 \quad (5)$$

$$\begin{aligned} \frac{1}{\varepsilon} \frac{\partial U}{\partial \tau} + \frac{1}{\varepsilon^2} (U \frac{\partial U}{\partial X} + V \frac{\partial U}{\partial Y}) = -\frac{\partial P}{\partial X} + \frac{v_{nf}}{\alpha_f \varepsilon} \nabla^2 U - \frac{v_{nf}}{\alpha_f} \frac{U}{Da} \\ - \frac{F_c}{\sqrt{Da}} U \sqrt{U^2 + V^2} + \frac{\beta_{nf}}{\beta_f} Ra Pr \sin \gamma \theta \end{aligned} \quad (6)$$

$$\begin{aligned} \frac{1}{\varepsilon} \frac{\partial V}{\partial \tau} + \frac{1}{\varepsilon^2} (U \frac{\partial V}{\partial X} + V \frac{\partial V}{\partial Y}) = -\frac{\partial P}{\partial Y} + \frac{v_{nf}}{\alpha_f \varepsilon} \nabla^2 V - \frac{v_{nf}}{\alpha_f} \frac{V}{Da} \\ - \frac{F_c}{\sqrt{Da}} V \sqrt{(\frac{\alpha_f}{L} U)^2 + (\frac{\alpha_f}{L} V)^2} + \frac{\beta_{nf}}{\beta_f} Ra Pr \cos \gamma \theta \end{aligned} \quad (7)$$

$$\frac{\partial \theta}{\partial \tau} + U \frac{\partial \theta}{\partial X} + V \frac{\partial \theta}{\partial Y} = \frac{\alpha_{nf}}{\alpha_f} \nabla^2 \theta + \frac{\alpha_{nf}}{\alpha_f} Q \theta \quad (8)$$

The initial and boundary conditions:

$$\begin{aligned} \tau = 0 : U = V = 0, \theta = 0, 0 \leq Y \leq 1 \\ \tau > 0 : U = V = 0, \theta = 1, X = 0, 0 \leq Y \leq 1 \\ U = V = 0, \theta = 0, X = 1, 0 \leq Y \leq 1 \\ U = V = 0, \frac{\partial \theta}{\partial Y} = 0, Y = 0 \& 1, 0 \leq Y \leq 1 \end{aligned}$$

And the non-dimensional parameters are defined by,

$$\begin{aligned} Da = \frac{K}{L^2}, \quad Pr = \frac{v_f}{\alpha_f}, \quad Ra = \frac{g \beta_f L^3 (Th - Tc)}{v_f \alpha_f}, \\ \sigma = \frac{\varepsilon (\rho C_p)_{nf} + (1 - \varepsilon) (\rho C_p)_s}{(\rho C_p)_{nf}}, \quad Q = \frac{q L^2}{(\rho C_p)_{nf} \alpha_{nf}} \end{aligned}$$

## 2.2 Numerical analysis

COMSOL Multiphysics is used to solve the isotherms and streamlines for parameters inclination angle at  $0^\circ$ ,  $45^\circ$ ,  $90^\circ$ ,  $135^\circ$  and  $180^\circ$ . COMSOL Multiphysics is a software tool for finite element analysis to simulate and analyze physical processes in a variety of engineering and scientific fields. The main reference has a verified steady state solution because all the three residuals  $U$ ,  $V$  and  $\theta$  have been met at the same time and are smaller than the value of  $10^{-5}$ .

**Table 2** Utilizing practical models to formulate properties of nanofluids

| Properties of nanofluids      | Utilized model  |
|-------------------------------|---|
| Density                       | $\rho_{nf} = (1-\varphi)\rho_f + \varphi\rho_p$   |
| Thermal diffusivity           | $\alpha_{nf} = \frac{k_{nf}}{(\rho c_p)_{nf}}$  |
| Thermal conductivity          | $\frac{k_{nf}}{k_f} = \frac{(k_p + 2k_f) - 2\varphi(k_f - k_p)}{(k_p + 2k_f) + \varphi(k_f - k_p)}$ |
| Heat capacitance              | $(\rho c_p)_{nf} = (1-\varphi)(\rho c_p)_{nf} + \varphi(\rho c_p)_p$                                |
| Thermal expansion coefficient | $(\rho\beta)_{nf} = (1-\varphi)(\rho\beta)_{nf} + \varphi(\rho\beta)_p$                             |
| Dynamic viscosity             | $\mu_{nf} = \frac{\mu_{nf}}{(1-\varphi)^{2.5}}$   |

Table 2 represented utilizing practical models to formulate properties of nanofluids. The formula for density, thermal diffusivity, thermal conductivity, heat capacitance, thermal expansion coefficient and dynamic viscosity will be used to find the value for each term. Other previous studies were done in heat transfer and fluid in worldwide according to various fields of studies [12, 13].

## 3. Result and discussion

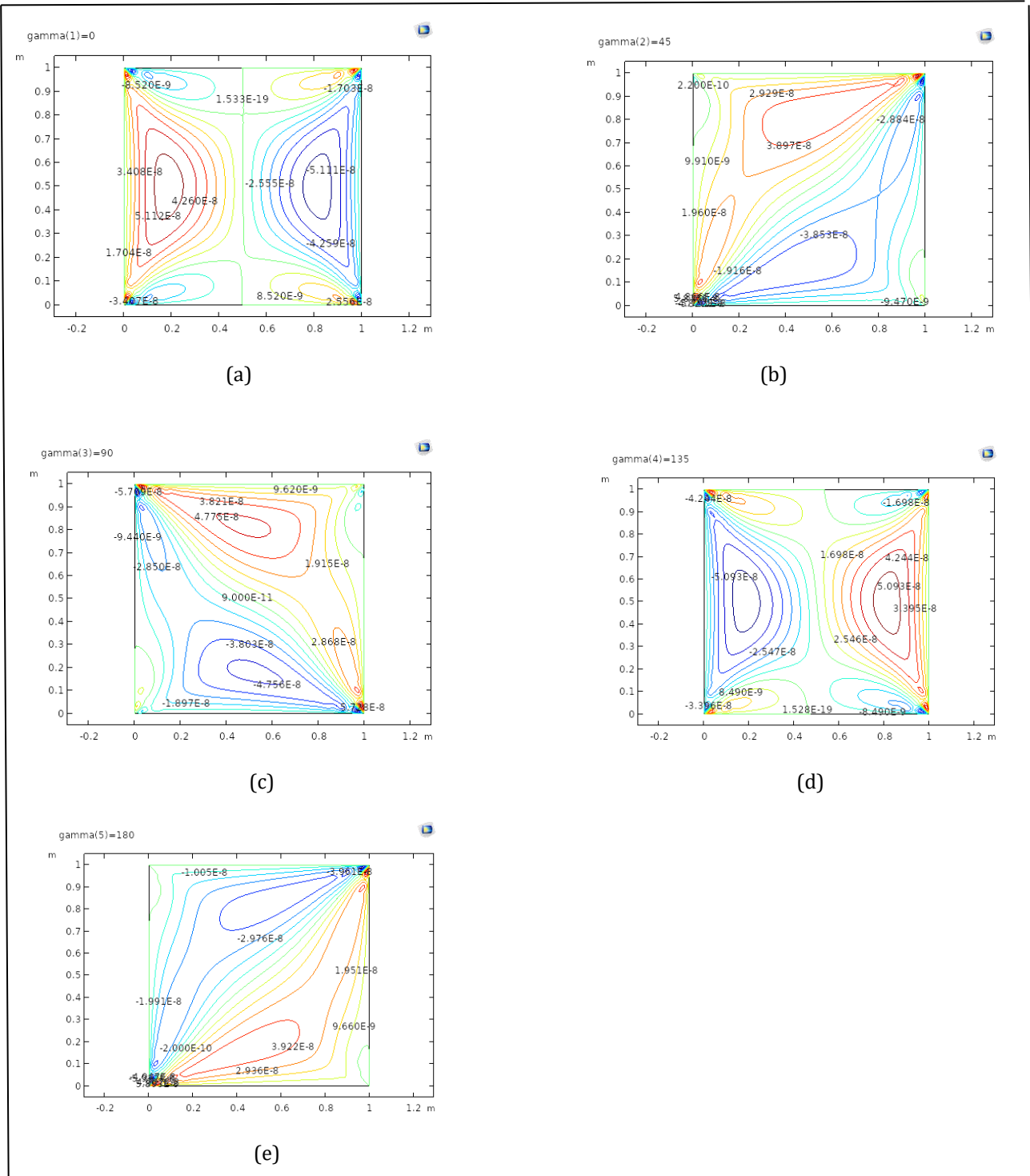
### 3.1 Streamlines

Fig 2 show the inclination angle from  $0^\circ$  to  $180^\circ$ . For the (a), it exhibits clockwise rotational motion, contributing to the overall complexity of fluid dynamics in the cavity. In addition, each angle of the figure reveals subtle and localized movement, adding a very slightly different to the fluid flow characteristics. A deliberate rearrangement of the hot and cold walls is observed with the hot wall placed on the left and the cold wall on the right. The strategic repositioning distribution and heat transfer dynamics in the cavity. Movement toward the left and right sides introduces a directional component to the flow, thereby shaping the overall thermal behavior.

Next, for (b), the cavity moves  $45^\circ$ , introducing a shift in its orientation. At the same time, the hot and cold walls, important components that affect heat transfer, are moved to the top and bottom at an angle of  $45^\circ$  oppositely. In the rotated cavity, a distinctive double circulation cell pattern emerges, exhibiting two separate flow cells exhibiting two separate flow cells exhibiting complex interactions. The direction of these cells, either clockwise or counterclockwise, adds a dynamic layer to the fluid dynamics. This contrasts with the findings in inclination angle  $0^\circ$  outlining the effect of altered boundary conditions on fluid flow patterns. Cavity and wall repositioning prompts an interesting consideration of potential implications for heat transfer efficiency and fluid mixing. This observation opens up space for further exploration, inviting questions about how certain parameters can be manipulated to obtain diverse flow patterns in the system.

Fig 2 (c) shows a different configuration where the cavity undergoes a  $45^\circ$  rotation, accompanied by a strategic relocation of the hot and cold walls to the upper right and lower left, also at an angle of  $45^\circ$ . The intricate interactions between the two circulation cells introduce a dynamic aspect to fluid flow, suggesting complex and organized movement. Drawing parallels with previous inclination angle  $45^\circ$ , it becomes clear that subtle changes in cavity orientation and wall position can significantly affect the observed flow patterns. The observed double circulation cell pattern prompts further investigation of its implications for heat transfer

efficiency and fluid dynamics in the system, providing valuable insights for a broader understanding of the described phenomenon.



**Fig. 2** Streamlines for inclination angle (a)  $\gamma=0^\circ$ , (b)  $\gamma=45^\circ$ , (c)  $\gamma=90^\circ$ , (d)  $\gamma=135^\circ$ , (e)  $\gamma=180^\circ$

Besides for Fig 2 (d), the streamlines are clearly visible at a gamma angle of  $135^\circ$ , revealing different fluid flow patterns in the cavity. In the middle center of the diagram, the cavity is filled with cells circulating in a clockwise direction, indicating dynamic and orderly fluid movement. These central circulation cells contribute to the complexity of the entire strip. In addition, at each corner of the figure, there is a visible but smaller movement, introducing local variations to the fluid flow characteristics. Notably, the hot and cold walls have been strategically rearranged, with the hot walls moved to the right and the cold wall to the left.

Lastly, for Fig 2 (e) reveals a distinctive configuration in which the cavity undergoes a  $45^\circ$  rotation, facilitated by a clockwise circulating cell. The rotational transformation is accompanied by a strategic relocation

of the hot wall to the lower right and the cold wall to the upper left. Clockwise circulating cells within the cavity suggest dynamic fluid movement, adding an interesting dimension to the overall flow pattern.

From all the streamlines above, we can conclude that double circulation cell configurations cause heat transfer to be more efficient. It is because double circulation cells create a more complex and organized flow pattern within the cavity. The mixing of the liquid in the cavity increases due to the two circulating cells moving in opposite directions.

### 3.2 Isotherms

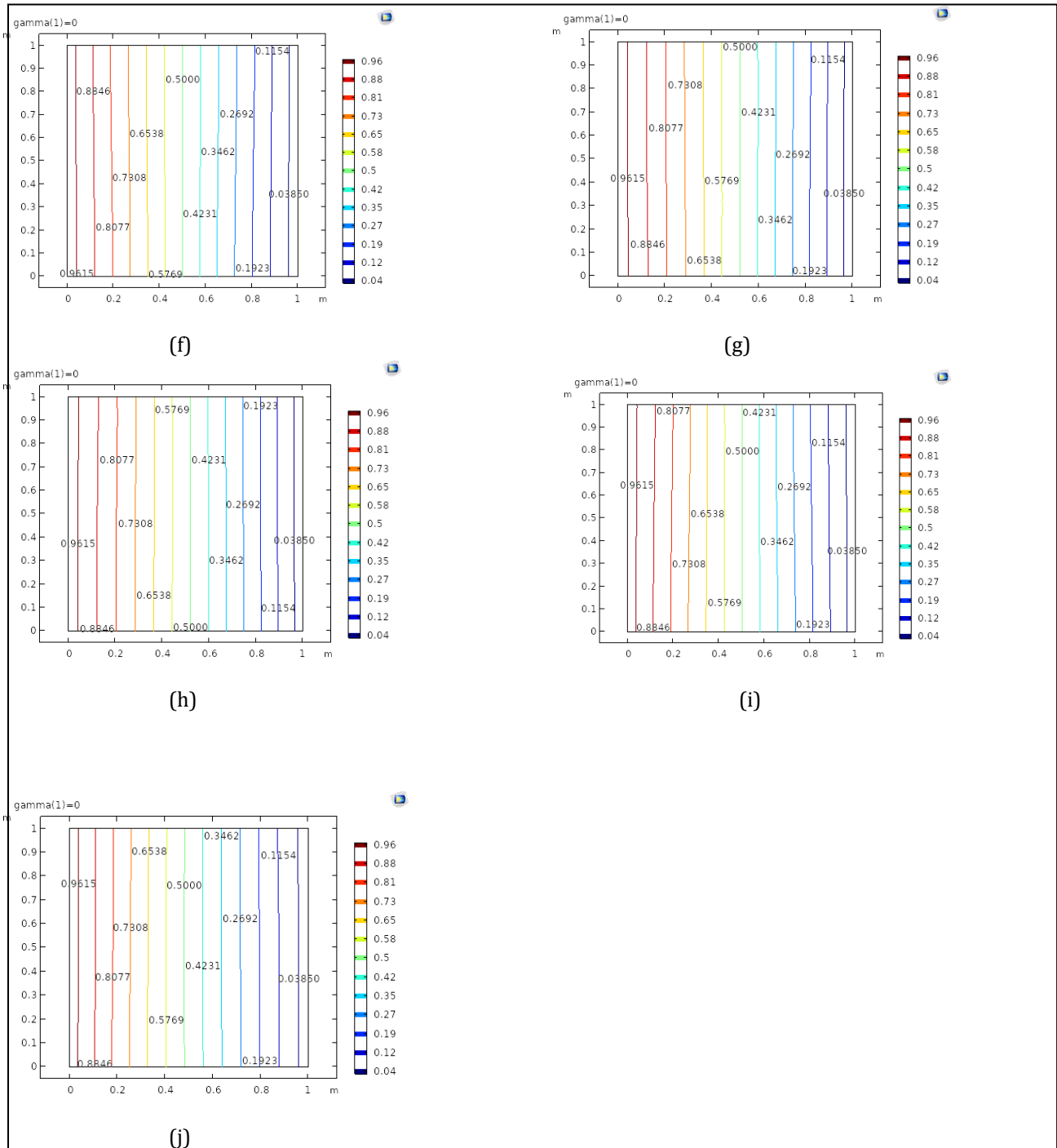


**Fig. 3** Isotherms for inclination angle (f)  $\gamma=0^\circ$ , (g)  $\gamma=45^\circ$ , (h)  $\gamma=90^\circ$ , (i)  $\gamma=135^\circ$ , (j)  $\gamma=180^\circ$

To conclude Fig 3, the isotherms is fixed which is  $10^{-3}$  and different inclination angle range from  $0^\circ$  to  $180^\circ$  are shown. The temperature distribution shows cold temperatures on the right and hot temperatures on the left. The observed shift in isotherm levels points to a systematic shift in temperature from hot to cold throughout the system under study. The findings provide insights into the impact of inclination angle variations on temperature distribution and heat transfer within fluid dynamics of the system. Due to the pressure at all inclination angles being the same, there is only a slight change in all isotherms. The values on the isotherm are all different but the hot and cold positions are the same.

The shape of the isotherm remains unchanged despite using different values of the angle of inclination is because the isotherms describe the relationship between the concentration of the solid and the liquid, which is used to absorption process. In this context, the isotherm does not depend on the angle of the inclination, but rather on the relationship between the solid and fluid concentrations at constant temperature. Therefore, although the value of the tilt angle may be different, the isotherm still describes the same relationship between the solid and fluid concentrations at constant temperature. This shows that the isotherm is dependent on the relationship between solid and fluid concentrations at constant temperature, rather than on the angle of inclination.

#### 4. Conclusion

This study presents the results of isotherms and streamlines of natural convection heat transfer. It has been done to examine the impact of several non-dimensional characteristics, including heat generation, inclination angle and Darcy number. Five different value of gamma which are  $0^\circ$ ,  $45^\circ$ ,  $90^\circ$ ,  $135^\circ$  and  $180^\circ$  used in this study. Each of these values produces a different effect in the form of streamlines and isotherms. The following interesting findings are provided by the study's effective completion.

The streamlines change according to the magnitude of the inclination angle and the variety of wall positions that are rich in fluid dynamics in the cavity. Double circulation cell configurations can cause heat transfer to be more efficient. For isotherms, the temperature field and fluid flow are not significantly affected by adding nanoparticles in the base fluid. The same shape of the isotherm is because the isotherms describe the relationship between the concentration of the solid and the liquid which is used to absorption process.

#### Acknowledgement

The authors would thank the Faculty of Applied Sciences and Technology, Universiti Tun Hussein Onn Malaysia for its support.

#### Conflict of Interest

Authors declare that there is no conflict of interests regarding the publication of the paper.

#### Author Contribution

The authors confirm contribution to the paper as follows: **study conception and design, data collection, analysis and interpretation of results:** Nur Haidah Izzati Abu and Muhamad Ghazali Kamardan; **draft manuscript preparation:** Nur Haidah Izzati Abu and Muhamad Ghazali Kamardan. All authors reviewed the results and approved the final version of the manuscript.

#### References

- [1] Yao, H. (1999). Studies of natural convection in enclosures using the finite volume method.
- [2] Bhanvase, B., & Barai, D. (2021). *Nanofluids for Heat and Mass Transfer*. Elsevier. <https://doi.org/10.1016/C2019-0-03241-4>
- [3] Giwa, S. O., Adeleke, A. E., Mohsen Sharifpur, & Meyer, J. P. (2023). *From 2007 to 2021*. 174, 63-174. <https://doi.org/10.1016/b978-0-323-90498-8.00001-4>
- [4] Sojoudi, A., Saha, S. C., & Gu, Y. T. (2015). Natural convection due to differential heating of inclined walls and heat source placed on bottom wall of an attic shaped space. *Energy and Buildings*, 89, 153-162, <https://doi.org/10.1016/j.enbuild.2014.12.042>
- [5] Acharya, S. (1985). Natural convection in an inclined enclosure containing internal energy sources and cooled from below. *International Journal of Heat and Fluid Flow*, 6(2), 113-121. [https://doi.org/10.1016/0142-727X\(85\)90045-1](https://doi.org/10.1016/0142-727X(85)90045-1)
- [6] Soong, C.-Y., Tzeng, P.-Y., Chiang, D. C., & Sheu, T.-S. (1996). Numerical study on mode-transition of natural convection in differentially heated inclined enclosures. 39(14), 2869-2882. [https://doi.org/10.1016/0017-9310\(95\)00378-9](https://doi.org/10.1016/0017-9310(95)00378-9)



- [7] Baytaş, A. C. (2000). Entropy generation for natural convection in an inclined porous cavity. *International Journal of Heat and Mass Transfer*, 43(12), 2089–2099.  
[https://doi.org/10.1016/S0017-9310\(99\)00291-4](https://doi.org/10.1016/S0017-9310(99)00291-4)
- [8] Wang, Q. W., Zeng, M., Huang, Z. P., Wang, G., & Ozoe, H. (2007). Numerical investigation of natural convection in an inclined enclosure filled with porous medium under magnetic field. *International Journal of Heat and Mass Transfer*, 50(17-18), 3684–3689.  
<https://doi.org/10.1016/j.ijheatmasstransfer.2007.01.045>
- [9] Fatih S., Oztop, H. F., & Khaled Al-Salem. (2014). Natural convection of ferrofluids in partially heated square enclosures. *Journal of Magnetism and Magnetic Materials*, 372, 122–133.  
<https://doi.org/10.1016/j.jmmm.2014.07.058>
- [10] Saleh, H., Alsabery, A. I., & Hashim, I. (2015). Natural convection in polygonal enclosures with inner circular cylinder. *Advances in Mechanical Engineering*, 7(12), 168781401562289-168781401562289.  
<http://dx.doi.org/10.1177/1687814015622899>
- [11] Rajarathinam, M. & Nithyadevi. N. (2017). Heat transfer enhancement of Cu-water nanofluid in an inclined porous cavity with internal heat generation. *Thermal Science and Engineering Progress*, 4, 35–44.  
<https://doi.org/10.1016/j.tsep.2017.08.003>
- [12] Ibrahim, M. H. R., & Aman, F. (2022). Analysis on Hiemenz flow over a shrinking sheet in hybrid nanofluid. *Enhanced Knowledge in Sciences and Technology*, 2(1), 221-230.
- [13] Azmi, M. A., & Aman, F. (2022). Analysis on hybrid nanofluid over a shrinking sheet with transpiration and uniform shear flow. *Enhanced Knowledge in Sciences and Technology*, 2(1), 210-220.